Two-photon interference in a standard Mach-Zehnder interferometer

Y. H. Shih, A. V. Sergienko, M. H. Rubin, T. E. Kiess,* and C. O. Alley*
Department of Physics, University of Maryland, Baltimore County, Baltimore, Maryland 21228
(Received 29 December 1992; revised manuscript received 2 September 1993)

A pair of light quanta with different colors (155.9-nm difference in center wavelength) generated from parametric down-conversion was injected collinearly into one input port of a Mach-Zehnder interferometer. Coincidence interference behavior was studied over a wide range of optical path differences of the interferometer. A measurement of 75% interference visibility with oscillation of the pump frequency for a large optical path difference of the interferometer (43 cm) is the signature of a quantum two-photon entangled state, which reflects both particle and wave nature of the light quanta in one experiment.

PACS number(s): 42.50.Wm, 03.65.Bz

When a single photon beam is injected into a Mach-Zehnder interferometer with two detectors placed in two output ports, first-order (first order in intensity, second order in field) and second-order (second order in intensity, fourth order in field) interference phenomena are understood both classically and quantum mechanically. However, when a two-photon beam generated from optical parametric down-conversion is directed into a Mach-Zehnder interferometer, some of the second-order interference phenomena only can be explained by quantum mechanics.

We report a two-photon interference experiment in which a pair of photons with different colors ($\lambda_1 = 632.8$ nm and $\lambda_2 = 788.7$ nm, a 155.9-nm difference in center wavelength) was directed to *one input port* of a Mach-Zehnder interferometer. Two detectors were used in the two output ports of the interferometer for direct counting and for coincidence counting with the help of a 300-psec coincidence time window. The interference behavior was studied for a wide range of the optical-path differences of the interferometer, from the white-light condition $\Delta L \cong 0$ to about $\Delta L \cong 127$ cm ($\cong 2\times 10^3$ times of the coherence length of the down-converted beams). In one experiment both the particle and the wave nature of the light quanta were clearly demonstrated. This experiment is a continuation of our previous research [1].

The experimental arrangement is shown in Fig. 1. A 10-cm-long type-I phase-matching potassium dihydrogen phosphate crystal pumped by a single-mode 351.1-nm cw argon-ion laser line is used to generate collinear photon pairs at wavelengths of 632.8 and 788.7 nm. The coherence length of the pump beam was measured to be longer than 5 m. The 351.1-nm pump beam and the down-converted beams were polarized in the extraordinary and ordinary ray directions of the crystal, respectively. A Glan-Thompson prism was used to separate the collinear down-converted photon beams from the orthogonal polarized 351.1-nm pump beam. Before the 351.1-nm laser line was sent to pump the parametric down-conversion, a quartz dispersion prism was used to separate out the radiation lines of the laser plasma tube which are close to the 632.8- and 788.7-nm wavelengths. It is important to isolate the detectors from directly viewing these radiation lines which cannot be blocked by the spectral filters.

The collinear 632.8- and 788.7-nm photon pair was then injected into a standard Mach-Zehnder interferometer composed of 50%-50% beam splitters (BS) and mirrors. The optical-path differences of the interferometer $\Delta L = L - S$ can be arranged to be shorter or longer than the coherence length l_{coh} of each beam of the down-conversion field and the coincidence time window $c\Delta T_{\text{coin}}$. The collinear photon pairs were injected onto the beam splitter with an incident angle of about 10°–12° (near normal), for which the reflected and transmitted intensities of the 632.8- and 788.7-nm beams were measured to be equal (50%-50%) within 5%. No significant absorption losses were measured for these dielectric coat-

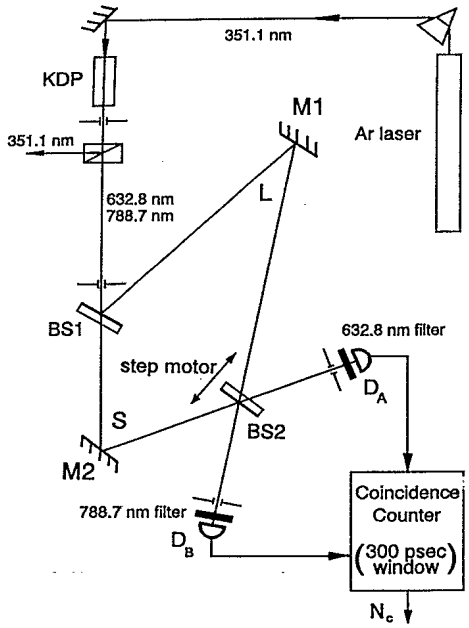

FIG. 1. Schematic diagram of the experiment.

*Permanent address: Department of Physics, University of Maryland, College Park, MD 20742.

ing beam splitters.

Two Geiger mode avalanche photodiode detectors, operated at dry-ice temperature, were used to record coincidences in the two output ports of the Mach-Zehnder interferometer. Two narrow-band interference spectral filters, with central wavelengths 632.8 and 788.8 nm, mounted with detectors A and B, respectively, were aligned to receive the down-converted light quanta at normal incidence. The spectral bandwidths are 1.4 and 1.7 nm for the 623.8- and 788.7-nm spectral filters, respectively.

The 800-mV output pulses from detector A and detector B were sent to counter N_1, N_2, and a coincidence circuit to record the coincidences. The coincidence time window ΔT_{coin} was about 300 psec. The direct counts N_1 and N_2 of the detectors D_A and D_B, respectively, and the coincidence counts N_c of the 300-psec time window, were recorded by a 386 personal computer which was also used for the fine control of the step for changing the position of the beam splitter.

We collected data for three regions of interest. In the first region, $\Delta L < l_{\text{coh}}$, i.e., the optical-path differences of the interferometer are equal to within the first-order coherence length of the signal and idler. In the second region, $l_{\text{coh}} < \Delta L < c\Delta T_{\text{coin}}$. In the third region, $\Delta L > c\Delta T_{\text{coin}}$. The following reported data are all directly measured values without any noise reductions or theoretical corrections.

The first region $\Delta L < l_{\text{coh}}$. Figure 2 shows the normalized counting rate of N_c when the optical-path difference changed from the white-light condition to abut 5 μm. In this region, N_1 and N_2 both showed clear single wavelength, 632.8 and 788.7 nm, respectively, first-order interference patterns. However, N_c shows a complicated interference pattern with 632.8 and 788.7 nm and the beating and the sum frequencies. The interference visibility is close to 100% with the 300-psec coincidence window. The solid curve in Fig. 2 is a theoretical fitting of Eq. (9), discussed later. Figure 3 shows the typical interference patterns of N_c at $\Delta L \cong 115$ μm. The N_c pattern in Fig. 3 is different than that in Fig. 2 in two ways: (a) the interference visibility is reduced and (b) the beating component and the 632.8- and 788.7-nm components of the oscillation are reduced and the sum-frequency oscillation becomes predominant. The solid line in Fig. 3 is a theoretical curve resulting from Gaussian spectral filter functions in Eq. (9) of the following.

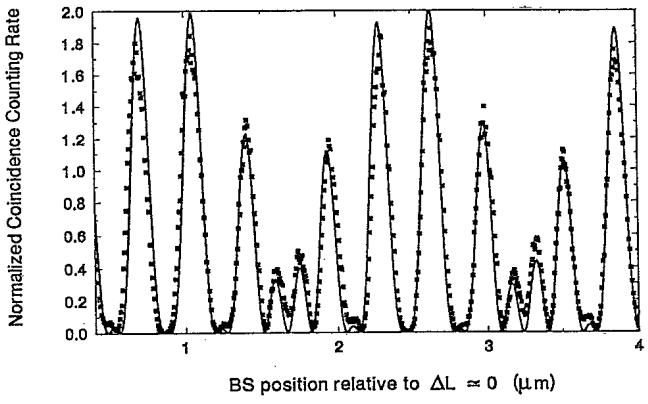

FIG. 2. Normalized coincidence counting rate of N_c at a near-white-light condition ($\Delta L \cong 0$). The beating frequency, with a 3.2-μm period, and sum frequency, with a 351.1-nm period, are evident from the graph. Signal and idler frequencies, at periods of 632.8 and 788.7 nm, also contribute. The solid line is a theoretical curve of Eq. (9).

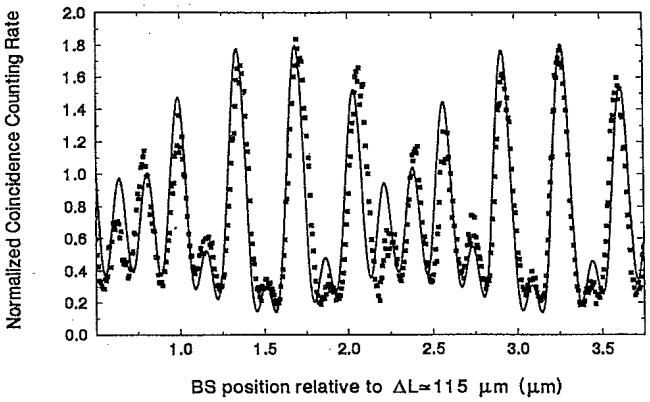

FIG. 3. Normalized coincidence counting rate of N_c at $\Delta L \cong 115$ μm. Compared with Fig. 2, the beating component and the ω_1 and ω_2 components of the modulation are reduced and the sum-frequency modulation becomes predominant. The solid line is a theoretical curve resulting from Gaussian spectral distributions in Eq. (9).

The second region $l_{\text{coh}} < \Delta L < c\Delta T_{\text{coin}}$. In this region both N_1 and N_2 became constant; however, N_c shows clear interference with the sum frequency. Figure 4 shows the interference pattern of N_c for $\Delta L \cong 0.5$ cm. Compare to the 300-psec coincidence time window and the coherent length of the down-converted beams, which satisfies $l_{\text{coh}} < \Delta L < c\Delta T_{\text{coin}}$. The interference visibility is (44±3)% with oscillation at a wavelength of 351.1 nm only. In this region, all the measured interference patterns have modulation visibilities close to but less than 50%.

The third region $\Delta L > c\Delta T_{\text{coin}}$. The interference patterns of N_c in the final region of interest $\Delta L > c\Delta T_{\text{coin}}$ is

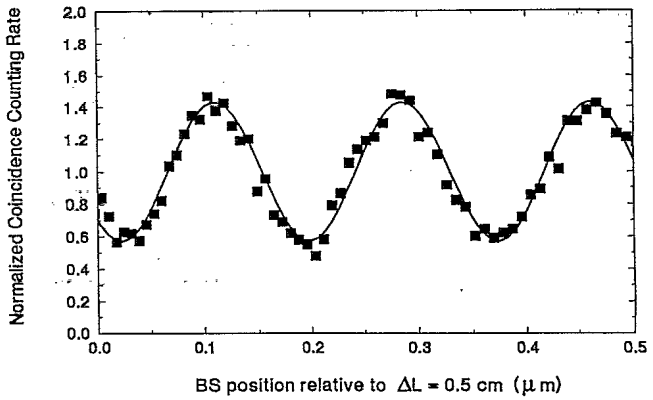

FIG. 4. Normalized coincidence counting rate of N_c at $\Delta L \cong 0.5$ cm for a $\Delta T_{\text{coin}} = 300$ psec time window. The beating modulation and the ω_1 and ω_2 modulations have completely disappeared. A visibility of (44±3)% was measured.

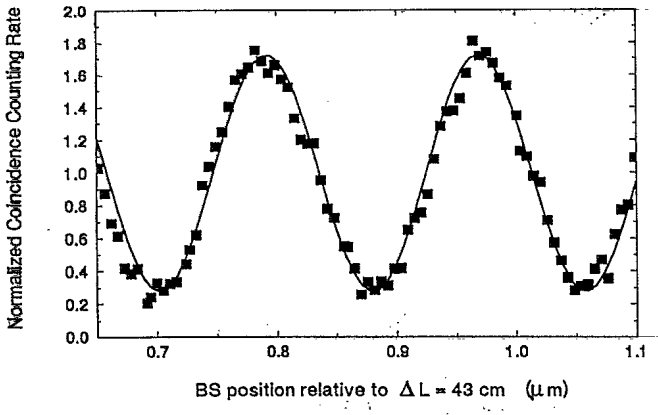

FIG. 5. Normalized coincidence counting rate of N_c at $\Delta L \cong 43$ cm for a $\Delta T_{\text{coin}} = 300$ psec time window. The observed (75±3)% interference visibility marks the quantum interference effect. The modulation at $\lambda = 0.351$ μm is the sum frequency of the signal and idler light quanta.

presented in Fig. 5. An interference visibility of (75±3)% was measured at $\Delta L \cong 43$ cm with an interference period of 351.1 nm. When ΔL increased to about 127 cm, the interference visibility was measured to be (56±3)%. In this region, no interference oscillations were found for N_1 and N_2.

In an earlier paper [2] a general theory for a two-photon interference experiment in two interferometers, first suggested by Franson [3], was developed. The theory of this experiment is similar. We refer readers to that paper for details. The coincidence counting rate is calculated from the field fourth-order correlation function:

$$G(\mathbf{r}_1 t_2, \mathbf{r}_2 t_2; \mathbf{r}_2 t_2, \mathbf{r}_1 t_1) = \langle E_1^{(-)} E_2^{(-)} E_2^{(+)} E_1^{(+)} \rangle , \quad (1)$$

where $E_j^{(+)}$ is the positive-frequency part of the electric field in the Heisenberg picture evaluated at position $\mathbf{r}_j$ and time t_j. $E_j^{(-)}$ is the Hermitian conjugate of $E_j^{(+)}$ and the expectation value is the trace over the initial state of the system. The average coincidence counting rate is given by

$$R_c = \frac{1}{T} \int \int_{-T/2}^{T/2} dt_1 dt_2 G(\mathbf{r}_1 t_2, \mathbf{r}_2 t_2; \mathbf{r}_2 t_2, \mathbf{r}_1 t_1) \times S(t_1 - t_2, \Delta T_{\text{coin}}) , \quad (2)$$

where $S(t, \Delta T_{\text{coin}})$ is a coincidence detection function, ΔT_{coin} is the coincidence time window, and the integrals are over the detection time T. The detectors may be taken as point detectors located at $\mathbf{r}_1$ and $\mathbf{r}_2$. A two-photon amplitude can be defined at the detectors by

$$\Psi(t_1, t_2) = \langle \text{vac} | E_1^{(+)}(t_1) E_2^{(+)}(t_2) | \Psi \rangle , \quad (3)$$

where

$$E_j^{(+)}(t_j) \int d\omega f_j(\omega) e^{-i\omega t} a_j(\omega) , \quad (4)$$

a_j is the destruction operator of the photons in the jth beam, and f_j is the pass band of the filter in the beam peaked at Ω_j. We take $\Omega_1 + \Omega_2 = \omega_p$, as the pump frequency. In this experiment the widths of the filters Ω_1 and Ω_2 are chosen so that each detector only detects one of the down-converted beam, i.e., $\Omega_1 - \Omega_2 \gg \sigma$, the bandwidth of the filters.

The two-photon part of the state that emerging from the down-conversion crystal may be taken to be

$$\Psi = \int \int d\omega_1 d\omega_2 \delta(\omega_1 + \omega_2 - \omega_p) a_1^\dagger(\omega_1) a_2^\dagger(\omega_2) | \text{vac} \rangle , \quad (5)$$

where the δ function indicates a perfect frequency phase-matching condition. The wave-number phase-matching condition is implicit in the choice of the location of the pinholes and the detectors. In the usual way (3) can be rewritten as

$$\Psi(t_1, t_2) = A(t_1, t_2) + A(t_1 - \Delta T, t_2 - \Delta T) + A(t_1, t_2 - \Delta T) + A(t_1 - \Delta T, t_2) , \quad (6)$$

where $\Delta L = c \Delta T$ is the optical-path difference in the two arms of the interferometer. The first (second) term is the amplitude for which both photons follow the short (long) path through the interferometer and the third (fourth) term is the amplitude for which the photon ω_1 follows the short (long) path and photon ω_2 which follows the long (short) path. A simple calculation using Gaussian filters

$$f_j = \exp[-\omega - \Omega_j)^2 / 2\sigma_j^2] , \quad (7)$$

where σ_j is the bandwidth of the filter, gives

$$A(t_1, t_2) = \exp[-i(\Omega_1 t_1 + \Omega_2 t_2)] u(t_1 - t_2) , \quad u(t) = K \exp[-\Sigma^2 t^2 / 2] , \quad 1/\Sigma^2 = 1/\sigma^2 + 1/\sigma^2 , \quad (8)$$

where K is a constant. We note in passing that Σ determines the bandwidth of the detected wave packets.

If we now substitute Eqs. (6) and (7) into (2), the average counting rate may be written in the form

$$R_c = R_0 [J_0 + J_1 \cos(\Omega_1 \Delta T) + J_1 \cos(\Omega_2 \Delta T) + J_+ \cos(\Omega_1 \Delta T - \Omega_2 \Delta T) + J_- \cos(\Omega_1 \Delta T + \Omega_2 \Delta T)] . \quad (9)$$

The J's are explicitly defined by integrals in [2]. If we take

$$S(t, \Delta T_{\text{coin}}) = \exp(-|t| / 2\Delta T_{\text{coin}}) , \quad (10)$$

all the integrals can be written in terms of error functions erfc. Define $\Lambda = 1/(4\Sigma \Delta T_{\text{coin}})$; then

$$\begin{aligned} J_0 &= C[2\text{erfc}(\Lambda) + \exp(-\Delta T / 2\Delta T_{\text{coin}}) \text{erfc}(\Lambda + \Sigma \Delta T / 2) \\ &\quad + \exp(-\Delta T / 2\Delta T_{\text{coin}}) \text{erfc}(\Lambda - \Sigma \Delta T / 2)] , \\ J_1 &= 2C \exp(-\Sigma^2 \Delta T^2 / 4) \\ &\quad \times [\exp(-\Delta T / 4\Delta T_{\text{coin}}) \text{erfc}(\Lambda + \Sigma \Delta T / 2) \\ &\quad + \exp(-\Delta T / 4\Delta T_{\text{coin}}) \text{erfc}(\Lambda - \Sigma \Delta T / 2)] , \\ J_+ &= 2C \exp(-\Sigma^2 \Delta T^2) \text{erfc}(\Lambda / 2) , \\ J_- &= 2C \, \text{erfc}(\Lambda) , \end{aligned} \quad (11)$$

where C is a constant that need not concern us. We re-

mind the reader that $\mathrm{erfc}(x) \Longrightarrow 0$ as $x \Longrightarrow \infty$ and erfc $(x) \Longrightarrow 2$ as $x \Longrightarrow -\infty$. The key point to understand the behavior of the coincidence counting oscillation is the variation of the J's with the increase of $\Delta T = \Delta L/c$.

For $\Delta L < l_{\mathrm{coh}}$, $J_0 = J_1 = 2J_+ = 2J_-$. From (9), the coincidence counting rate R_c has oscillations at ω_1, ω_2, and their sum and difference frequencies. The visibility is 100% in this case. As seen in Fig. 2, the data are very well fit by (9) in this case. As ΔL increases, J_1 and J_+ rapidly decrease, becoming negligible when ΔL is approaching l_{coh}, the coherence length of the down-converted beam. This can be seen in Fig. 3, when $\Delta L = 115$ μm, which is about one-half of the coherence length l_{coh}, the beating component and the 632.8- 788.7-nm components of the oscillation are reduced, and the sum-frequency oscillations becomes predominant.

$l_{\mathrm{coh}} < \Delta L < c\Delta T_{\mathrm{coin}}$. As ΔL increases to be greater than l_{coh} both J_1 and J_+ are zero and we are left with

$$R_c = R_0[J_0 + J_- \cos(\Omega_p \Delta T)] , \tag{12}$$

which indicates that the oscillation is only at the sum frequency. The modulation visibility can only approach a maximum value of 50%; this is because the contribution of the last two terms in J_0 arise from the state amplitudes in which one photon follows the longer and the other the shorter path of the interferometer. Figure 4 clearly shows this oscillation.

$\Delta L > c\Delta T_{\mathrm{coin}}$. In this region, the interference pattern looks the same as in case (2), however, the interference visibility increases to more than 50%. This is because of the vanishing of the last two terms in J_0, the interference visibility is predicted to be 100% in idealized experimental conditions. This interference behavior is clearly demonstrated in Fig. 5.

The above simple theory of the quantum-mechanical model provides a good quantitative understanding of what is happening in this experiment without the introduction of any artificial parameters. The key point is the variation of the J's. In the region of $\Delta L < l_{\mathrm{coh}}$, all J's contribute to the interference pattern, which is not distinguishable from a classical model. In this region the first-order interference pattern appears in both N_1 and N_2 counting. The first-order interference may be considered as the interference effect of each beam with itself. The coincidence oscillation may be explained as the result of the product of N_1 and N_2. When ΔL increases, J_1 and J_+ approach zero due to the vanishing of the factor $\exp(-\Sigma^2 \Delta T^2)$. This effect may be considered also to be a classical wave behavior. In the second region, $l_{\mathrm{coh}} < \Delta L < c\Delta T_{\mathrm{coin}}$, the coincidence interference behavior shown in (12) is expected. Since the ω_1 and ω_2 beams never meet at the same detector because of the filter and each beam does not interfere with itself when $\Delta L > l_{\mathrm{coh}}$, the coincidence oscillation is a non-local two-photon interference effect. In the third region, it is by now well known that under the condition $\Delta L > c\Delta T_{\mathrm{coin}}$, the interference is a purely quantum effect. It is impossible to have a classical model to explain the coincidence counting-rate oscillation of more than 50% visibility. Mathematically the increase of the visibility is due to the vanishing of the factor $\exp(-\Delta T/2\Delta T_{\mathrm{coin}})$ in J_0. Physically this is due to the cutoff by the coincidence time window of the state amplitudes in which one photon follows the longer path and other the shorter arm of the interferometer, which indicates the particle nature of the photon. This is equivalent to the projection of a quantum entangled state [4,5]

$$\Psi(t_1,t_2) = A(t_1,t_2) + A(t_1 - \Delta T, t_2 - \Delta T) \tag{13}$$

from the initial state. For $\Delta L > c\Delta T_{\mathrm{coin}}$, the quantum entangled two-photon state (13) is realized by the measurement, which reflects both the particle and the wave nature of the light quanta in one experiment. This makes the interference phenomenon, which is characterized by a visibility of more than 50% with a oscillation frequency of the pump field, manifestly quantum.

Note added. After this paper was submitted a related experiment by Larchuk *et al.* appeared in Phys. Rev. Lett. [6].

We would like to thank J. D. Franson for useful discussions. This work was supported in part by the Office of Naval Research Grant No. N00014-91-J-1430.

[1] Y. H. Shih, A. V. Sergienko, and M. H. Rubin, Phys. Rev. A **47**, 1288 (1993).

[2] M. H. Rubin and Y. H. Shih, Phys. Rev. A **45**, 8138 (1992).

[3] J. D. Franson, Phys. Rev. Lett. **62**, 2205 (1989).

[4] E. Schrödinger, Naturwissenschaften **23**, 807 (1935); **23**, 823 (1935); **23**, 844 (1935). A translation of these papers appears in *Quantum Theory and Measurement*, edited by J. A. Wheeler and W. H. Zurek (Princeton University Press, Princeton, 1983).

[5] M. A. Horne, A. Shimony, and A. Zeilinger, Phys. Rev. Lett. **62**, 2209 (1989).

[6] T. S. Larchuk, R. A. Campos, J. G. Rarity, P. R. Tapster, E. Jakeman, B. E. A. Saleh, and M. C. Teich, Phys. Rev. Lett. **70**, 1603 (1993).